Chemical Science

Dynamic Article Links ►

Cite this: DOI: 10.1039/c0xx00000x

www.rsc.org/xxxxxx

EDGE ARTICLE

Absolute Redox Potential of Liquid Water: A First-Principles Theory

Michael Lucking, Yi-Yang Sun*, Damien West, Shengbai Zhang*

Received (in XXX, XXX) Xth XXXXXXXXX 20XX, Accepted Xth XXXXXXXXX 20XX
DOI: 10.1039/b000000x

A first-principles molecular dynamic method is proposed to calculate the absolute redox potentials of liquid water. The key of the method is the evaluation of the difference between the vacuum level and the average electrostatic potential inside liquid water, which employs an average over both space and time. By avoiding the explicit use of the Kohn-Sham levels, such as the position of the valence band maximum, as the reference energy for the excited electrons, we are able to calculate water redox potentials accurately using a semi-local density functional and an entropic contribution estimated from experimental data.

Introduction

Oxidation-reduction potential (or redox potential) is a fundamental quantity in electrochemistry, which measures the tendency of a chemical species (an ion or a molecule) to gain or lose electrons to another species, typically in aqueous solutions. Standard hydrogen electrode (SHE) is the accepted standard, with respect to which the redox potentials of other species are measured.[1] The definition of SHE is based on the electrochemical half reaction

$$2H^+(aq) + 2e^- \rightarrow H_2(g) \qquad (1)$$

such that, in the SHE scale, the redox potential for hydrogen gas production from aqueous protons is zero. One can also define the redox potential with respect to the vacuum level (called absolute redox potential or E_{abs}).[2] The absolute hydrogen production potential, $E_{abs}(H^+/H_2)$, is intimately related to the proton hydration energy, $\Delta G_{hyd}(H^+)$, which is also an important fundamental quantity determining, e.g., the acidity constant (or the *p*Ka value) of a chemical species in aqueous solution.[3] The two quantities are connected through the Born-Haber cycle, as illustrated in Fig. 1, namely, the sum of $E_{abs}(H^+/H_2)$ and $\Delta G_{hyd}(H^+)$ equals to the sum of the atomization free energy of hydrogen molecules and ionization free energy of hydrogen atoms.

Not only is E_{abs} essential in the fundamental definitions mentioned above, but it is also necessary in determining other physicochemical properties when aqueous solution is involved. Currently, photocatalytic splitting of water into hydrogen fuel using semiconductor electrodes is a highly pursued approach to converting solar energy to chemical energy. In a semiconductor-based photoelectrochemistry setup, E_{abs} with respect to the band edge positions of the semiconductor electrodes measures the ability for a reaction to move forward. For example, for hydrogen and oxygen production reactions to take place simultaneously and effectively, the semiconductor band edges should straddle the redox potentials for H_2 production, i.e., $E_{abs}(H^+/H_2)$, and O_2 production.[4]

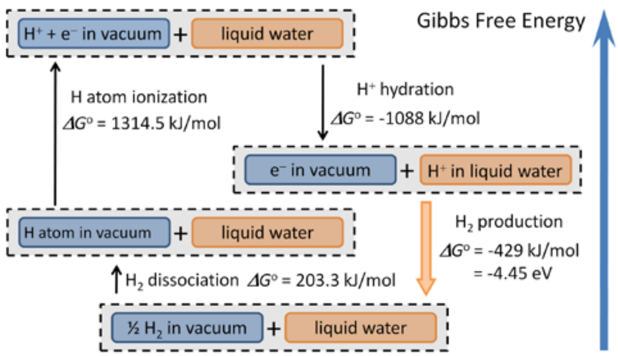

Fig. 1 Born-Haber cycle showing the relation between the proton hydration energy and the absolute hydrogen production potential.

Theoretical design has become a valuable approach to the search and optimization of semiconductor materials for water splitting.[5] The success of such an approach, however, relies critically on how accurately the theoretical calculations can reproduce the redox potentials. First-principles calculations, such as those based on the density functional theory (DFT),[6] have been widely used to study various material properties. Yet, the study on the redox potential using DFT is still challenging. This is partly because of the difficulty of first-principles methods dealing with the electrochemical reactions in a liquid solvent. Cluster models,[7] which may be combined with empirical methods such as those based on polarizable continuum models,[8] are the commonly used method in this context. In recent years, there has been important advancement in the calculation of redox potentials using DFT-based molecular dynamics (MD) under the periodic boundary condition (PBC).[9] So far, such theories have focused on the relative redox potential with respect to SHE. To calculate the absolute redox potential under the PBC, it is necessary to introduce an interface with vacuum into the calculation, for which there is still not a computationally viable approach. Additionally, there is the concern on the reliability of the DFT[10] because the method, in particular, the Kohn-Sham (KS) eigenvalues, suffers from the well-known band-gap errors.[11]

In this paper, we propose a method, based on first-principles MD simulations, to directly calculate the absolute redox potential without resorting to any Born-Haber cycles. Here, we focus on the hydrogen production reaction, but the method can be straightforwardly applied to other aqueous reactions where referencing to the vacuum level is required. We formulate E_{abs} in such a way that avoids the use of the KS eigenvalues for the reason mentioned above. We make use of the fact that the DFT method within the semi-local approximations is able to produce reasonably accurate electron charge density, and hence reasonably accurate electrostatic potential. We propose a space-time averaging scheme to calculate the difference between the vacuum level and the average electrostatic potential inside liquid water. Our calculated absolute hydrogen production potential is 4.37 eV below the vacuum level at room temperature, which is in good agreement with the recommended value of 4.44 eV based on experimental measurements,[2c] despite that our calculated KS band gap of liquid water is only 4.5 eV, which is considerably smaller than the experimental value of 6.9 eV.[12]

Results and discussion

We first rewrite Eq. (1), i.e., the H_2 production step in Fig. 1, as

$$H^+(aq) + e^-(g) \rightarrow \text{water} + \tfrac{1}{2}H_2(g). \qquad (2)$$

By having the electron in the vacuum (denoted by g throughout this paper), the change in the Gibbs free energy in Eq. (2) defines $E_{abs}(H^+/H_2)$ as

$$E_{abs}(H^+/H_2) = G(H^+(aq)) - G(\text{water}) - \tfrac{1}{2}G(H_2(g)) + eV_{vac}, \qquad (3)$$

where G(water), $G(H^+(aq))$, and $G(H_2(g))$ are the Gibbs free energies of pure water, a proton in water, and H_2 gas, respectively. The last term, eV_{vac}, is the potential energy of an electron of charge e at the vacuum level V_{vac}. In a cluster-model calculation, the eV_{vac} term can be conveniently set to zero. However, for bulk water calculated using a PBC as in the present case, this term needs to be evaluated explicitly. This is because V_{vac} and $G(H^+(aq))$ in Eq. (3) must have the same reference potential.

Using the relation $G=U+PV-TS$, Eq. (3) can be expressed as

$$\begin{aligned} E_{abs}(H^+/H_2) &= U(H^+(aq)) - U(\text{water}) - \tfrac{1}{2}U(H_2(g)) + eV_{vac} - T\Delta S \\ &\equiv \Delta U + eV_{vac} - T\Delta S. \qquad (4)\end{aligned}$$

Here, U(water), $U(H^+(aq))$ and $U(H_2(g))$ are the total energies of pure water, a proton in water, and an isolated H_2 molecule, respectively. We have ignored the contribution of the PV term, which is on the order of 0.01 eV. To evaluate $\Delta U + eV_{vac}$, we used first-principles MD simulations. The entropy contribution $T\Delta S$ can also be evaluated based on the MD simulations.[13] Reliable results, however, usually require simulations in nano-second scale, which are currently beyond the capability of our computer resources. In the present study, we adopted the available experimental results. The entropy term $T\Delta S$ is given by

$$\begin{aligned} T\Delta S &= TS(H^+(aq)) - TS(\text{water}) - \tfrac{1}{2}TS(H_2(g)) \\ &= TS(H^+(aq)) - TS(\text{water}) - TS(H^+(g)) + TS(H^+(g)) \\ &\quad - \tfrac{1}{2}TS(H_2(g)), \qquad (5)\end{aligned}$$

where the first three terms defines the proton hydration entropy, which is experimentally measured to be –0.40 eV at 298 K and 1 bar,[14] and the last two terms can be obtained using the standard database,[15] which gives +0.14 eV at 298 K and 1 bar. Thus, $T\Delta S$ = –0.26 eV were used.

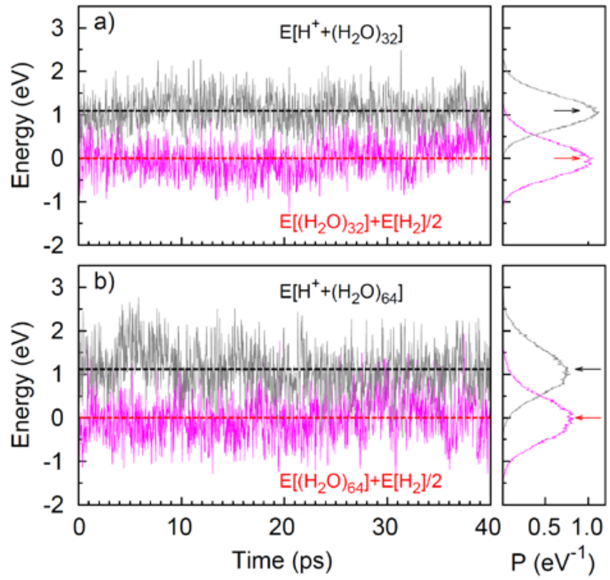

Fig. 2 MD simulations of pure water and proton hydration in water. (a) and (b) are for the results from using supercells containing 32 and 64 water molecules, respectively. The left panels show the potential energy evolution in the last 40 ps of the simulations. The right panels show the histograms of the potential energy, i.e., the probability density P. The gray lines are for the term $U(H^+(aq))$ in Eq. (4), while the pink lines are for the term $U(\text{water})+\tfrac{1}{2}U(H_2(g))$.

Our MD simulations were based on the DFT as implemented in the VASP program.[16] To evaluate the term ΔU in Eq. (4), we employed supercells containing 32 and 64 water molecules, respectively. The volume of the supercell was set according to the experimental density of water at room temperature (0.997 g/cm^3). For a cubic 64-molecule supercell, this corresponds to a length of 12.43 Å. The generalized gradient approximation of Perdew, Burke and Ernzerhof (PBE)[17] was used for the exchange-correlation functional. The ionic dynamics was based on the Newton's equation of motion using forces calculated with the Hellmann-Feynman theorem. We used projector augmented wave (PAW) potentials[18] to describe the core-valence interaction and planewaves up to kinetic energy of 340 eV as the basis set. The Brillouin zone was represented by the Γ point. Our simulations were conducted in the canonical ensemble using the Nosé thermostat[19] to control the temperature at 298 K. The time step was chosen to be 0.25 fs. Zero-point energy was not included in our MD simulation. With the above settings, it takes about 230 total CPU hours (Intel Xeon Nehalem 2.6 GHz) to perform 1 ps simulation using the 64-molecule supercell.

We obtain the liquid water structure by equilibrizing a randomized ice structure at 298 K in 80 ps simulation. We then inserted a proton into the water and carried out MD simulations for 60 ps. The evolutions of the potential energy (gray colored) in the last 40 ps are shown in Fig. 2, while the results in the first 20 ps are omitted because that period contains the equilibrization of the proton in water. To confirm that our pure water is reasonably equilibrized, we also continued the simulation of pure water for another 60 ps. The results in the last 40 ps are shown in Fig. 2 (pink colored), together with those of the proton. To obtain

$U(H^+(aq))$ and $U(water)+½U(H_2(g))$ in Eq. (4), we considered two different approaches: first, we took the average of the potential energy over the 40 ps (the left panels in Fig. 2); second, we generated a histogram from the MD simulation (the right panels in Fig. 2) and then fitted it to a Gaussian function. The values for ΔU in Eq. (4) evaluated from these two approaches (namely, dashed lines in the left panels and peaks in the right panels) agree to each other to within 0.01 eV. From the 64-molecule supercell, we obtained ΔU = 1.12 eV, while from the 32-molecule supercell, we obtained ΔU = 1.09 eV. It is expected that further increasing the supercell size will change the result by less than 0.03 eV.

The calculation of $U(H^+(aq))$ requires the use of a positively charged supercell. In order to remove the divergence in the electrostatic interaction of the periodic images of positive charges, we applied a uniform negative charge background in the supercell calculation. The fictitious interaction energy arising from the use of the PBC and the charge background can be estimated using a Madelung correction $½\alpha q^2/\varepsilon L$,[20] where α is the Madelung constant ($\alpha \approx 2.84$ for a cubic cell), q is the charge inserted to the supercell (q = 1 for H^+), ε is the static dielectric constant of liquid water ($\varepsilon \approx 80$ at room temperature), and L is the length of the supercell ($L \approx 12.43$ Å for a 64-molecule supercell). Thus, we obtain a Madelung correction of 0.02 eV to the total energy. Applying the correction to the result for 64-molecule supercell, we obtain ΔU = 1.14 eV. The Madelung correction typically overestimates the error due to the use of the uniform charge background[21] so that including higher-order terms will make the correction smaller.

Next, we evaluate eV_{vac} in Eq. (4). Note that if $E_{abs}(H^+/H_2)$ in Eq. (4) were calculated without the eV_{vac} term, then it has been assumed that the electron has a potential energy equal to the reference energy of the H^+-in-water supercell, which is usually taken as the average electrostatic potential of the entire supercell in a planewave-based code.[22] This implies that the correct V_{vac} should be the difference between the vacuum level and this reference energy. In the dilute limit, the average electrostatic potential of the H^+-in-water supercell can be approximated by that of the corresponding charge neutral supercell of pure water. This allows us to calculate V_{vac} using the supercell setup shown as an inset in Fig. 3(a), which contains both a bulk-like water region in a slab geometry and a vacuum region. In such a geometry, V_{vac} is simply the difference between the average potentials in the two regions. For crystalline materials, it is usually straightforward to obtain V_{vac} using the slab geometry. For liquids, however, there is still not a scheme in the literature for averaging inside the bulk. In addition, the water slab always exhibits a macroscopic dipole along the direction perpendicular to the slab/vacuum interface, resulting in a tilted electrostatic potential in the vacuum region. This tilted vacuum potential can be made flat by flipping over the water slab about the center of the slab and averaging the potentials from the unflipped and flipped slabs.

In principle, if one can perform a sufficiently long time MD simulation on the slab geometry, the electrostatic potentials in both the bulk water and vacuum regions should be flat due to the averaging of the water slab configurations over time evolution. However, we found that such a converged result cannot be obtained in currently affordable simulation time. So, the question is how to generate a series of water slabs that can effectively sample the configuration space. Instead of the time average, we propose a space-time average scheme, where we generate a series of slab supercells, as illustrated in the inset of Fig. 3(a), with the geometry of the water region taken from a snapshot of the bulk-water simulation. The spatial averaging is accomplished by first dividing the cubic supercell of the snapshot into N slices along, for example, the z direction, as shown in Fig. 3(b). Then, the slices from i to $i+N$ are used to build a water slab by appending a vacuum region. In this process, H atoms always follow the O atoms that they are bonded to. We can build N different slab supercells in this way by taking i from 1 to N. The electrostatic potentials for all these slab supercells are calculated and then averaged. This spatial averaging is repeated for a series of other snapshots extracted from the bulk-water simulation.

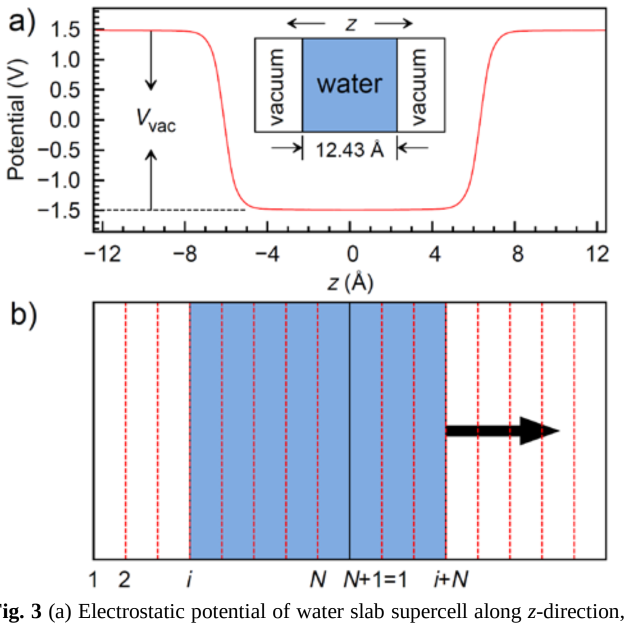

Fig. 3 (a) Electrostatic potential of water slab supercell along z-direction, which is averaged over the xy-plane. The inset shows a schematic of the supercell setup, where the water region is a cubic region. Because of the periodicity in the xy-plane, the water region forms a slab, which is separated from its periodic images by vacuum regions. (b) shows the scheme for performing the spatial averaging based on a supercell obtained from a snapshot from the MD simulation on bulk water. Two cubic supercells are shown.

The final space-time averaged electrostatic potential along the z-direction is shown in Fig. 3(a), where we used N = 50 slices and 12 snapshots from 40 ps bulk-water simulation. The potentials for the last snapshot with i = 10, 20, 30, 40, and 50 are shown in Fig. 4(a). It can be seen that the potentials inside the water region have large fluctuations before the spatial averaging, which were commonly observed in previous studies,[23] while after the spatial averaging the potential becomes flat in both the water slab and vacuum regions. Fig. 4(b) shows the spatial-averaged potentials from all the 12 snapshots over 40 ps simulation time. It was found that the change in the potential over simulation time is rather small (within 0.1 V). Overall, the difference between the potentials in the vacuum and water region gives V_{vac}, as shown in Fig. 3(a), which is found to be 2.97 V.

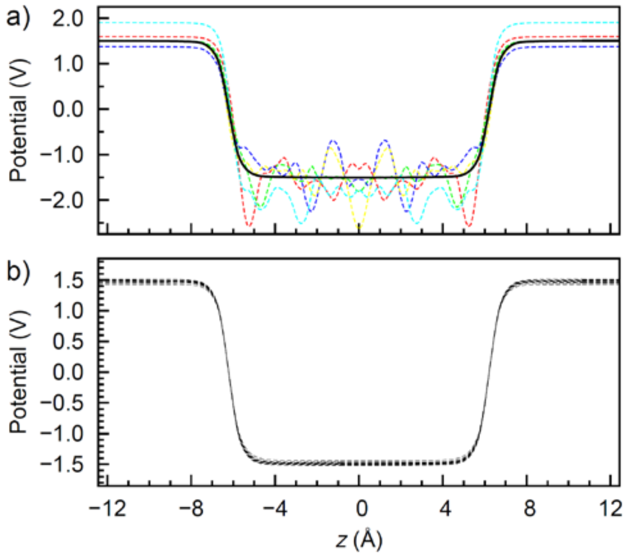

Fig. 4 (a) Electrostatic potentials of the water slab supercells used for spatial averaging, as illustrated in Fig. 3(b). The cases with i = 10, 20, 30, 40, and 50 are shown in dashed lines. The thick solid line shows the average from i = 1 to 50. (b) Spatial-averaged potentials for the water slab supercells generated from 12 snapshots over 40 ps MD simulation of bulk water.

Now, summing up ΔU (1.14 eV), eV_{vac} (2.97 eV), and $-T\Delta S$ (0.26 eV) following Eq. (4), we obtain $E_{abs}(H^+/H_2)$ = 4.37 eV below the vacuum level. Here, it is necessary to discuss the possible sources of error in our calculation. While the use of bulk-terminated water surface and the space-time average described above ensures the removal of surface dipole in our calculation, as evidenced by the vanishingly small change in V_{vac} in Fig. 4(b), a small dipole potential (0.1–0.2 V) may exist at real water/vacuum interface.[24] Another possible source of error is that the semi-local density functionals, such as PBE, often over-structure the liquid water.[25] It has been suggested that increasing the simulation temperature could empirically mitigate this effect.[25] We have performed MD simulation at 350 K obtaining ΔU = 0.99 eV. The change in ΔU reflects the fast kinetics at higher temperature that weakens the binding of proton in water. The eV_{vac} term, evaluated to be 2.94 eV at 350 K, is found relatively insensitive to the simulation temperature. Overall, the simulation at 350 K yields $E_{abs}(H^+/H_2)$ = 4.19 eV, about 0.18 eV lower than that at room temperature. Finally, it is worth mentioning that one may evaluate the pH value from first-principles using, e.g., the recently proposed microscopic theory.[26] Here, since the concentration of H^+ used in our calculation is close to the standard condition (i.e., 1 M concentration or about one H^+ per 55.5 water molecules), the error in our result related to the pH value is expected to be insignificant.

Experimentally, $E_{abs}(H^+/H_2)$ has been measured by several different approaches. An early experiment suggested a value of 4.73 eV, while two later experiments suggested values of 4.43–4.44 eV.[2] The value of 4.44 eV has been widely quoted in the literature, which was obtained by using the work function of metal Hg (4.50 V) and the standard potential difference (-0.0559 V) between a Hg electrode and a model SHE.[2c] Our calculated results are in reasonable agreement with experiment. Thus, by formulating the absolute redox potential without explicitly referring to any KS eigenvalues, our calculations establish the validity of using semi-local approximations, such as the PBE functional, to obtain reasonably accurate redox potentials through MD simulations for thermodynamic and electrochemical problems of ions in solvent. This could be a significant advantage over MD simulations using higher-level approximations such as the hybrid functionals, which are still computationally demanding.[27]

The theoretical calculation and experimental measurement of surface potential at water/vacuum interface have been discussed in several recent works.[23] The V_{vac} term here constitutes the majority of the surface potential. The possible missing part is the surface dipole potential as discussed above. The good agreement of our calculated redox potential with experiment suggests that the surface potential as discussed in the literature[23] could be measured by electrochemical methods with reasonable accuracy. In addition, our results also shed light on how to simulate solid/solution interface, which is a highly desirable objective. In particular, it shows that much of the chemistry of the solvated ions can be adequately described by the semi-local functionals. However, the result for an interface will suffer from the replacement of eV_{vac} in our formulation by the chemical potential of electrons at either the conduction band minimum or the valence band maximum of the solid, as they are KS eigenvalues. These are single-particle levels for which the corrections can be calculated by static higher-order methods. It is reasonable to expect that the corrections can also be empirically instated into the MD simulations to yield correct physics.

Conclusions

A first-principles molecular dynamics method is proposed to calculate the absolute redox potential. Using a space-time averaging scheme, we are able to calculate the difference between the vacuum level and the average electrostatic potential of liquid water. By avoiding the explicit use of the KS eigenvalues such as the position of the valence band maximum for the excited electron, we were able to calculate water redox potentials. The results using the PBE functional are in good agreement with experiment. We attribute the success of the method to the reasonably accurate charge density given by DFT under the local or semi-local approximation. This establishes the validity to apply these highly effective and efficient approaches to study both the energetics and dynamics of the more complex solid/solution systems.

Acknowledgements

YYS acknowledges support from US National Science Foundation under Award No. DMR-1104994. ML, DW and SBZ were supported by US Department of Energy (DOE) under Grant No. DE-SC0002623. The supercomputer time was provided by National Energy Research Scientific Computing Center (NERSC) under DOE Contract No. DE-AC02-05CH11231 and the Center for Computational Innovations (CCI) at Rensselaer Polytechnic Institute.

Notes and references

Department of Physics, Applied Physics & Astronomy, Rensselaer Polytechnic Institute, Troy, NY 12180, USA. Fax: +1 518 2766680; Tel: +1 518 2763643; E-mail: suny4@rpi.edu, zhangs9@rpi.edu.

1 A. J. Bard and L. R. Faulkner, *Electrochemical Methods: Fundamentals and Applications*, John Wiley & Sons, New York, 2001.

2 (a) R. Gomer and G. Tryson, *J. Chem. Phys.* 1977, **66**, 4413-4424; (b) H. Reiss and A. Heller, *J. Phys. Chem.* 1985, **89**, 4207-4213; (c) S. Trasatti, *Pure Appl. Chem.* 1986, **58**, 955-966.

3 C. Lim, D. Bashford, and M. Karplus, *J. Phys. Chem.* 1991, **95**, 5610-5620.

4 M. Grätzel, *Nature* 2001, **414**, 338-344.

5 (a) P. Wang, Z. Liu, F. Lin, G. Zhou, J. Wu, W. Duan, B.-L. Gu, and S. B. Zhang, *Phys. Rev. B* 2010, **82**, 193103; (b) Y. Gai, J. Li, S.-S. Li, J.-B. Xia, and S.-H. Wei, *Phys. Rev. Lett.* 2009, **102**, 036402; (c) W. Zhu, et al., *Phys. Rev. Lett.* 2009, **103**, 226401; (d) A. Walsh, K.-S. Ahn, S. Shet, M. N. Huda, T. G. Deutsch, H. Wang, J. A. Turner, S.-H. Wei, Y. Yana and M. M. Al-Jassim, *Energy Environ. Sci.* 2009, **2**, 774-782; (e) I. E. Castelli, T. Olsen, S. Datta, D. D. Landis, S. Dahl, K. S. Thygesena, and K. W. Jacobsen, *Energy Environ. Sci.* 2012, **5**, 5814-5819.

6 (a) P. Hohenberg and W. Kohn, *Phys. Rev.* 1964, **136**, B864-B871; (b) W. Kohn and L. J. Sham, *Phys. Rev.* 1965, **140**, A1133-A1138.

7 (a) W. Donald, R. Leib, J. O'Brien, M. Bush, and E. Williams, *J. Am. Chem. Soc.* 2008, **130**, 3371-3381; (b) G. Tawa, I. Topol, S. Burt, R. Caldwell, and A. Rashin, *J. Chem. Phys.* 1998, **109**, 4852-4863; (c) C. Zhan and D. Dixon, *J. Phys. Chem. A.* 2002, **106**, 9737-9744; (d) V. Bryantsev, M. Diallo, and W. Goddard III, *J. Phys. Chem. B.* 2008, **112**, 9709-9719; (e) J. Mejias and S. Lago, *J. Chem. Phys.* 2000, **113**, 7306-7316; (f) R. Jinnouchi, A. Anderson, *J. Phys. Chem. C.* 2008, **112**, 8747-8750; (g) A. Isse, A. Gennaro, *J. Phys. Chem. B.* 2010, **114**, 7894-7899; (h) C. P. Kelly, C. J. Cramer, and D. G. Truhlar, *J. Phys. Chem. B* 2006, **110**, 16066-16081.

8 J. Tomasi, B. Mennucci, and R. Cammi, *Chem. Rev.* 2005, **105**, 2999-3093.

9 (a) M. Sulpizi, S. Raugei, J. VandeVondele, P. Carloni, and M. Sprik, *J. Phys. Chem. B* 2007, **111**, 3969-3976; (b) M. Sulpizi and M. Sprick, *Phys. Chem. Chem. Phys.* 2008, **10**, 5238-5249; (c) J. Cheng, M. Sulpizi, and M. Sprik, *J. Chem. Phys.* 2009, **131**, 154504; (d) M. Mangold, L. Rolland, F. Costanzo, M. Sprik, M. Sulpizi, and J. Blumberger, *J. Chem. Theory Comput.* 2011, **7**, 1951-1961.

10 L. E. Roy, E. Jakubikova, M. G. Guthrie, and E. R. Batista, *J. Phys. Chem. A* 2009, **113**, 6745-6750.

11 L. J. Sham and M. Schlüter, *Phys. Rev. Lett.* 1983, **51**, 1888-1891.

12 J. V. Coe, A. D. Earhart, M. H. Cohen, G. J. Hoffman, H. W. Sarkas, and K. H. Bowen, *J. Chem. Phys.* 1997, **107**, 6023-6031.

13 H. Schäfer, A. E. Mark, W. F. van Gunsteren, *J. Chem. Phys.* 2000, **113**, 7809-7817.

14 W. A. Donald and E. R. Williams, *J. Phys. Chem. B* 2010, **114**, 13189-13200.

15 The NIST Chemistry WebBook, (http://webbook.nist.gov/).

16 G. Kresse and J. Furthmüller, *Comput. Mater. Sci.* 1996, **6**, 15-50.

17 J. P. Perdew, K. Burke, and M. Ernzerhof, *Phys. Rev. Lett.* 1996, **77**, 3865-3868.

18 G. Kresse and D. Joubert, *Phys. Rev. B* 1999, **59**, 1758-1775.

19 S. Nosé, *J. Chem. Phys.* 1984, **81**, 511-519.

20 M. Leslie and M. J. Gillan, *J. Phys. C* 1985, **18**, 973-982.

21 C. Freysoldt, J. Neugebauer, and C. G. Van de Walle, *Phys. Rev. Lett.* 2009, **102**, 016402.

22 J. Ihm, A. Zunger, and M. L. Cohen, *J. Phys. C* 1979, **12**, 4409-4422.

23 (a) K. Leung, *J. Chem. Phys. Lett.* 2010, **1**, 496-499; (b) S. M. Kathmann, I. W. Kuo, C.-J. Mundy, and G. K. Schenter, *J. Phys. Chem. B* 2011, **115**, 4369-4377.

24 (a) I. Benjamin, *Chem. Rev.* 1996, **96**, 1449-1475; (b) P. B. Petersen and R. J. Saykally, *Annu. Rev. Phys. Chem.* 2006, **57**, 333-364; (c) K. B. Eisenthal, *Chem. Rev.* 1996, **96**, 1343-1360.

25 (a) J. VandeVondele, F. Mohamed, M. Krack, J. Hutter, M. Sprik, and M. Parrinello, *J. Chem. Phys.* 2005, **122**, 014515; (b) M. V. Fernández-Serra and E. Artacho, *J. Chem. Phys.* 2004, **121**, 11136-11144; (c) S. Yoo, X. C. Zeng, and S. S. Xantheas, *J. Chem. Phys.* 2009, **130**, 221102; (d) C. Zhang, T. A. Pham, F. Gygi, and G. Galli, *J. Chem. Phys.* 2013, **138**, 181102; (e) Y. Zhao, H. Li, and X. C. Zeng, *J. Am. Chem. Soc.* 2013, **135**, 15549-15558.

26 Y.-H. Kim, K. Kim, and S. B. Zhang, *J. Chem. Phys.* 2012, **136**, 134112.

27 C. Zhang, D. Donadio, F. Gygi, and G. Galli, *J. Chem. Theory Comput.* 2011, **7**, 1443-1449.